

Trimmed-diamond Shaped Toggle Magnetoresistive Random
Access Memory Cells

G. Mankey – University of Alabama

et al.

Deposited 07/09/2019

Citation of published version:

Fukuma, Y., et al. (2009): Trimmed-diamond Shaped Toggle Magnetoresistive Random Access Memory Cells. *Journal of Applied Physics*, 105(7).

DOI: <https://doi.org/10.1063/1.3104788>

Trimmed-diamond shaped toggle magnetoresistive random access memory cells

Cite as: J. Appl. Phys. **105**, 073916 (2009); <https://doi.org/10.1063/1.3104788>

Submitted: 16 October 2008 . Accepted: 19 February 2009 . Published Online: 08 April 2009

Y. Fukuma, H. Fujiwara, P. B. Visscher, and G. J. Mankey



View Online



Export Citation

ARTICLES YOU MAY BE INTERESTED IN



[The design and verification of MuMax3](#)

AIP Advances **4**, 107133 (2014); <https://doi.org/10.1063/1.4899186>

[Excitation of coherent propagating spin waves in ultrathin CoFeB film by voltage-controlled magnetic anisotropy](#)

Applied Physics Letters **111**, 052404 (2017); <https://doi.org/10.1063/1.4990724>

A horizontal banner for Alluxa. On the left, the Alluxa logo (a stylized 'A' with a blue and orange swirl) is next to the word 'Alluxa' in white. To the right of 'Alluxa' is the text 'YOUR OPTICAL COATING PARTNER' in white. Further right is a blue arrow pointing right, followed by the text 'DOWNLOAD THE LIDAR WHITEPAPER' in orange and white.

 Alluxa YOUR OPTICAL COATING PARTNER  DOWNLOAD THE LIDAR WHITEPAPER

Trimmed-diamond shaped toggle magnetoresistive random access memory cells

Y. Fukuma,^{a)} H. Fujiwara, P. B. Visscher, and G. J. Mankey
 MINT Center, University of Alabama, Tuscaloosa, Alabama 35487, USA

(Received 16 October 2008; accepted 19 February 2009; published online 8 April 2009)

We have performed micromagnetic simulations for the design of toggle magnetoresistive random access memory (MRAM) cells to make the operating field as low as possible while keeping a reasonable margin and thermal stability. The memory cells are composed of weakly coupled synthetic antiferromagnets. The cells are diamond-shaped to suppress the formation of edge domains, which increase the operating field. The adverse effect of the diamond shape making the remanent state too stable is prevented by trimming the sharp points. The optimization of the trimming allows us to reduce the operating field and offer a pathway for realizing high-density toggle MRAM. © 2009 American Institute of Physics. [DOI: 10.1063/1.3104788]

I. INTRODUCTION

The invention of the toggle-writing scheme by Savtchenko *et al.*¹ has helped solve the write margin problem of the conventional Stoner–Wohlfarth writing scheme in magnetoresistive random access memory (MRAM), leading to a successful introduction of MRAM into the market.² However, in order to further increase the memory density, it is imperative to reduce the start field H_{start} , the lowest field at which toggle switching occurs. In toggle MRAM, the free layer consists of a synthetic antiferromagnet (SAF), often elliptically shaped to create an easy magnetization direction by shape anisotropy. The word and digit pulse fields are applied sequentially at $\pm 45^\circ$ with respect to the easy axis of the magnetic anisotropy of the memory element. When the first word field is applied, the two magnetizations of SAF make a scissors configuration from the antiparallel configuration, so the total magnetization becomes nonzero. The pulse sequence [Fig. 1(b)] causes the total external field to rotate, and we can find a range of the pulse height within which the total magnetization rotates and at the end of the pulse sequence both magnetizations are reversed. We will refer to the lower and higher limits of the range as the start field H_{start} and the end field H_{end} , respectively. According to the analytical/numerical calculation based on the single domain model,^{3–7} to reduce H_{start} the total antiferromagnetic coupling between the two ferromagnetic layers comprising the SAF should be made very small; the antiferromagnetic magneto-static coupling is drastically increased by decreasing the dimension of the memory cell, so the exchange coupling should be zero or slightly ferromagnetic. It has also been shown that lowering the memory cell aspect ratio (length/width) will decrease H_{start} and increase the end field H_{end} for toggle switching, increasing the operating field margin (the difference between H_{start} and H_{end}).

Recent experimental results have demonstrated that the critical fields, H_{start} and H_{end} , are in surprisingly good agreement with those predicted by the single domain model, with

the exception of the writeability problem for a memory cell with low aspect ratio, e.g., circular cylinder, suggesting non-single-domain effects.⁸ Our micromagnetic simulations have shown that the formation of edge domains causes an increase in H_{start} in a relatively low aspect ratio range, supporting the above suggestion.⁹ Therefore, although an optimal solution based on the single domain model can be found in circular or elliptic shapes with aspect ratio of ≤ 1 with sufficiently large write margin as well as low H_{start} ,^{4,7} some measure is necessary to put the low aspect ratio into a practical use. In this paper, we provide a new approach for reducing H_{start} : a trimmed-diamond (TD) shaped cell, which is a diamond in

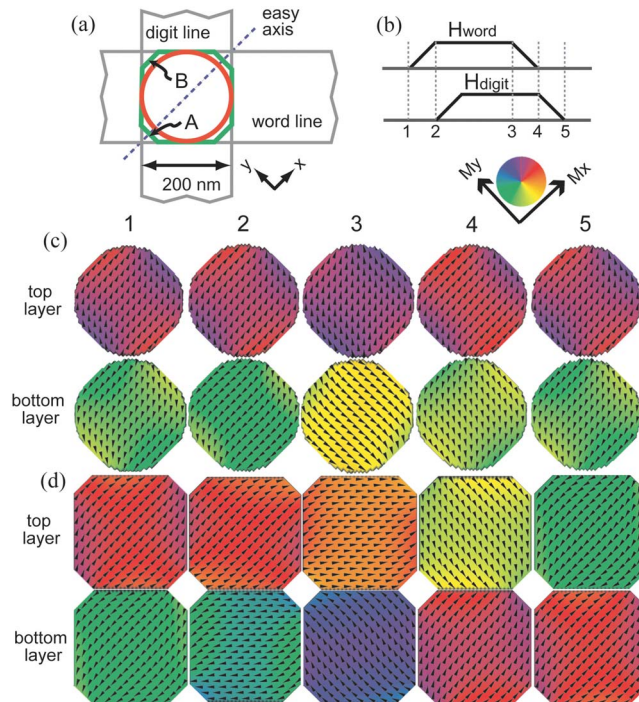


FIG. 1. (Color online) (a) Schematic diagram illustrating memory cell design for toggle MRAM. Magnetic moment configurations of (c) circular cylinder and (d) TD ($A=B=45$ nm) cells for toggle switching at 100 Oe.

^{a)}Present address: Advanced Science Institute, RIKEN, 2-1 Hirosawa, Wako 351-0198. Electronic mail: yfukuma@riken.jp.

which the sharp points are trimmed off, prevents the formation of edge domains and reduces H_{start} while keeping enough write margin and thermal stability.

II. MODEL

The memory cell design is performed by using a commercial micromagnetic simulator, “LLG.”¹⁰ We consider a memory cell with a magnetic tunnel junction composed of a SAF free layer structure combined with an ideal reference layer structure designed to produce no substantial stray field. Thus, only the free layer structure is modeled here. The magnetic layers of the SAF are assumed to be of CoFe with a saturation magnetization of 1200 emu/cm^3 , a uniaxial anisotropy of $1.8 \times 10^4 \text{ erg/cm}^3$ (intrinsic anisotropy field of $\sim 30 \text{ Oe}$), and an exchange constant of $1.6 \times 10^{-6} \text{ erg/cm}$. The thicknesses of the top and bottom layers are 2.4 and 2.5 nm, respectively. The slight thickness difference is to ensure that the first relaxation process from a saturated state yields a unique antiparallel initial state. After the relaxation, a toggle-writing operation is started. The interlayer exchange coupling constant J of the SAF is set to be zero or weakly ferromagnetic ($J=0.03 \text{ erg/cm}^2$), assuming a 5.0 or 3.0 nm thick intermediate nonmagnetic layer.¹¹ Each magnetic layer is discretized into a small mesh of $5 \text{ nm} \times 5 \text{ nm} \times t$ (t is the thickness of each magnetic layer) for the micromagnetic simulations. To compare the micromagnetic simulation results with the single domain model, the simulations are quasistatic: the Gilbert damping constant is large (0.2), and relatively long field pulses of 3 ns duration and 1 ns rise/fall times are assumed for the toggle-writing operation. The operation is supposed to be performed by consecutively applying a word field pulse and a digit field pulse with equal amplitudes [Fig. 1(b)].

III. RESULTS AND DISCUSSION

Figure 1(a) shows a schematic diagram of the cell design for toggle MRAM. The word and digit lines are located at $\pm 45^\circ$ with respect to the easy axis (x -axis) of the memory cell. The lengths of the cells along the word and digit lines are fixed at 200 nm. Here, for the TD cell, the trimmed edge lengths L_{trim} , denoted by A and B , are set equal to 45 nm. Figures 1(c) and 1(d) show the magnetization configuration of the top and bottom layers of SAF with $J=0$ during the toggle-switching process at the pulse field of 100 Oe for the circular cylinder and TD cells. The initial state is generated by relaxing magnetic moments, at zero field, from saturation in the 80° direction with respect to the easy axis. In the circular cylinder cell, clear edge domains are formed at both ends of the diagonals in the easy axis direction, making an S state in each layer at the remanent state, as is seen from the blue and yellow areas formed in the mainly red and green top and bottom layers, respectively, while in the TD cell only slight traces of the edge domains are seen to be formed. Figures 2(a) and 2(b) show schematically how the magnetic moments are aligned in the edge domains with respect to those in the central area at the initial state for the circular cylinder and TD cells, respectively. The edge domains of the top and bottom layers are antiparallel to reduce the magne-

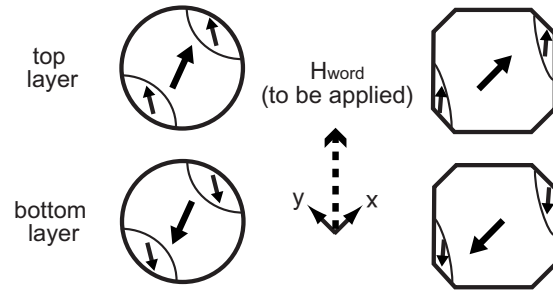


FIG. 2. Schematic illustration of the edge domains at the initial state 1 in Figs. 1(c) and 1(d) showing the arrangement of the magnetic moments in the edge domains relative to those in the main area of each layer cell.

tostatic energy, which stabilizes the edge domains. When the first word field is applied to the circular cylinder cell, the torque exerted on to the bottom moment is not strong enough to make sufficient clockwise rotation for toggle switching because of the loss of the net moment component perpendicular to the word field H_{word} caused by large deflection of the net moment from the easy axis direction. The counterclockwise torque exerted on the edge domains may further enhance the adverse effect on the toggle switching. This causes a counterclockwise rotation of the magnetization of the SAF at the next step when the digit field H_{digit} is added [step 3 in Fig. 1(c)], resulting in unsuccessful toggle switching by those fields of 100 Oe. For successful toggle switching, the magnetizations of the SAF form a scissors state from the antiparallel configuration after H_{word} is applied, and then the total magnetization rotates clockwise when H_{digit} is added. In the case of the TD cell, on the other hand, the formation of the edge domain is substantially suppressed at the initial state. Therefore, the same field sequence as applied to the circular cylinder cell causes the toggle-mode switching, as shown in Fig. 1(d).

The net moment of the initial state of each layer (normalized to the saturation moment) is a good index of the deviation from the single domain state. The moment is almost the same for both top and bottom layers and is shown in Fig. 3(a) as a function of trimmed edge length A (here we will set $A=B$) for the initial state. Figure 3(b) shows the critical fields for the toggle switching, H_{start} and H_{end} . The data obtained for the circular cylinder cell are also shown for reference. In the range of small trimming where the net moment M is almost constant, neither H_{start} nor H_{end} show a significant change. Then a sharp increase in H_{end} appears, accompanied by a slight decrease in H_{start} , reaching a minimum at around $A=B=45 \text{ nm}$. Finally, H_{end} tends to a plateau, and H_{start} slightly increases with further increase in trimming. These phenomena can be qualitatively explained as follows: for the diamondlike shape, the sharp points stabilize the initial configuration making H_{start} high, and H_{end} is rather low because the demagnetizing field at the edges preventing the saturation is low. The trimming relaxes the pinning of the edge moments of the diagonals in the easy axis direction, resulting in the reduction in H_{start} . As the trimming increases further, H_{start} starts to increase due to the formation of the S state. Figure 4 shows the demagnetizing field near the edge (at the center of L_{trim}) of the memory cells. Accord-

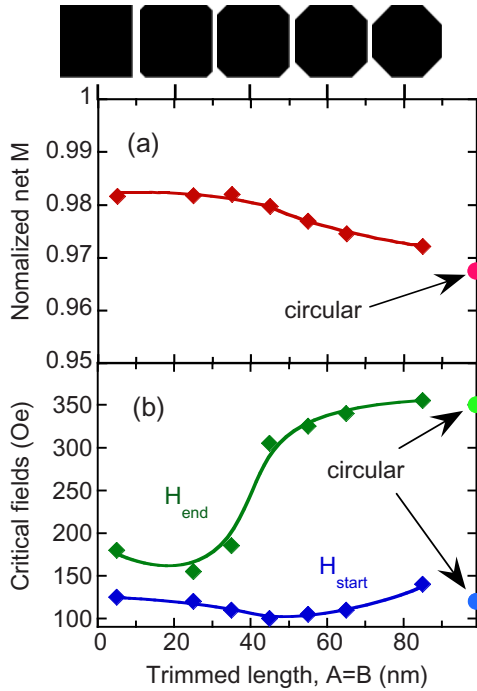


FIG. 3. (Color online) Trimmed edge length dependences of (a) normalized net moments and (b) critical fields for toggle switching in TD cells with 200 nm lengths.

ing to the single domain model,³⁻⁷ H_{end} corresponds to the saturation field of the SAF layer along the easy axis direction. As shown in Figs. 3 and 4, the behavior of H_{end} for the TD cell corresponds to that of the demagnetizing field because the saturation field is the field required for aligning the magnetic moments against the edge demagnetizing field. However, the increase in H_{end} as a function of the trimmed length is much greater than that of the edge demagnetizing field. The cells are clearly classified into two groups, one with low H_{end} and the other with high H_{end} . This is attributed to the change in the effect of the diagonal edges on the saturation with increasing L_{trim} . Figure 5 shows the magnetic moment distribution comparing two typical cases, one for small L_{trim} ($=5$ nm) and the other for large L_{trim} ($=45$ nm) at stage 3 in Fig. 1 (H_{digit} is applied after H_{word} is applied.) when intermediate operating field is applied. For $L_{trim} = 5$ nm, the moments at the edges along the x -axis (easy axis) direction are closer to the direction to be saturated than

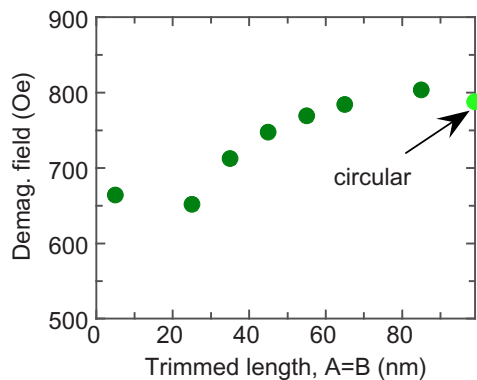


FIG. 4. (Color online) Trimmed edge length dependence of demagnetizing field in TD cells with 200 nm lengths.

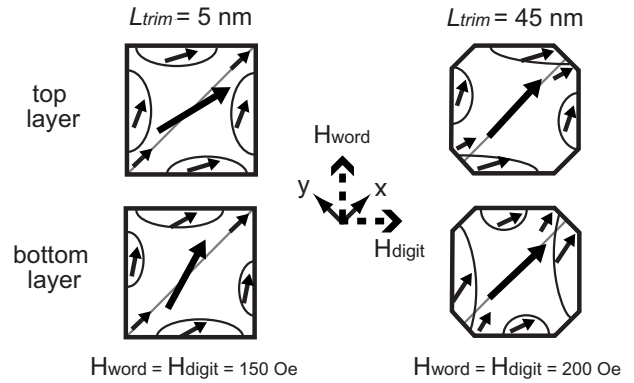


FIG. 5. Comparison of magnetic moment distribution between small and large trimmed length TD cells at the stage 3 (H_{digit} is applied after H_{word} is applied): the TD cells with $L_{trim} = 5$ nm and 45 nm are compared. Within the curved boundaries along the edges the moments are deflected from that of the center by greater than 15° . The thin solid lines running through the center moments are the diagonals parallel to easy axis direction (x -axis). The moment direction at the edges along the diagonals is also shown.

the moment at the center, while for $L_{trim} = 45$ nm they are retarding from saturation. That is, the effect of the diagonal edges changes from helping into preventing from saturation. This may cause the nonlinear dependence of H_{end} on the demagnetizing field at the diagonal edges mentioned above, although further detailed studies are necessary for the quantitative description of this behavior. As a consequence, to obtain a large write field margin, the edge of the sharp diamond must be trimmed. Thus, within our particular examples, a value of H_{start} as low as 100 Oe is attainable for $L_{trim} = 45$ nm while keeping a reasonable write window, which is substantially smaller than H_{start} of 120 Oe for the circular cylinder cell.

Figure 6 shows the aspect ratio dependence of H_{start} for elliptical cylinder and TD cells. In this simulation, the width of the cell [in the y -direction in Fig. 1(a), which is perpendicular to the easy axis] is fixed at 200 nm and the length (parallel to the easy axis) is changed from 200 to 240 nm. The trimmed edge lengths A and B are fixed at 40 nm. Based on the single domain model, H_{start} can be expressed as

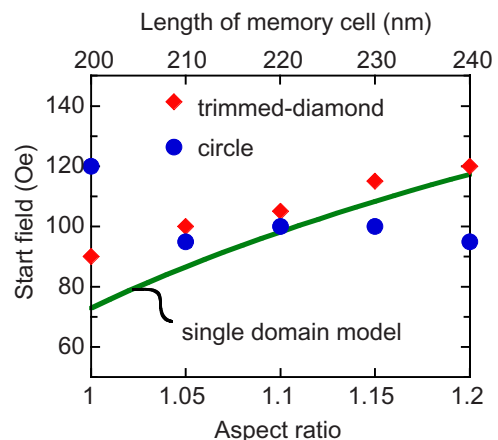


FIG. 6. (Color online) Aspect ratio dependence of toggle start field for elliptical cylinder and TD shaped cells. The line shows the single domain result.

$$H_{\text{start}} = H_{\text{flop}} / \sqrt{2}, \quad (1)$$

with

$$H_{\text{flop}} = \sqrt{H_k^* H_{\text{couple}} + H_k^* H_{k,\text{tot}}} \quad (H_{k,\text{tot}} \geq 0), \quad (2)$$

with

$$H_k^* = H_{K_u} + (1 - r)H_{K_{\text{sh}}}, \quad (3)$$

$$H_{k,\text{tot}} = H_{K_u} + H_{K_{\text{sh}}}, \quad (4)$$

where H_{K_u} is the induced intrinsic uniaxial anisotropy field, $H_{K_{\text{sh}}}$ is the shape anisotropy field, H_k^* is the effective anisotropy field representing the thermal stability of the SAF memory cell, r is the magnetostatic coupling attenuation factor, defined as the ratio of the average magnetostatic field due to one layer in the other layer to the average demagnetizing field in the first (source) layer, $H_{k,\text{tot}}$ is the total anisotropy field, which is the sum of the intrinsic uniaxial anisotropy field and the shape anisotropy field, and H_{couple} is the coupling field between two magnetic layers in the SAF including both interlayer exchange coupling and magnetostatic coupling. According to the single domain analysis, H_{start} will decrease with decreasing aspect ratio due to the decreases in H_k^* and $H_{k,\text{tot}}$. However, for the elliptic cylinder cell, H_{start} shows a complicated behavior due to the effect of the edge domains, as shown in Fig. 6, which is not a monotonic function of the aspect ratio. This may be attributed to the fact that the demagnetizing field at the edges of the diagonal in the easy axis direction increases with decreasing aspect ratio, which enhances the disturbing effect of the edge domains against the clockwise rotation of the bottom layer moment during the toggle-switching process. On the other hand, H_{start} of the TD cells decreases with decreasing aspect ratio as predicted by the single domain model. Therefore, the scaling behavior predicted by the single domain model will make a semiquantitative scaling guide for MRAM applications of TD cells.

With decreasing size of the memory cell, the magnetostatic coupling between magnetic layers comprising the SAF is increased, causing a drastic increase in H_{start} . Therefore, it is necessary to induce the ferromagnetic interlayer exchange coupling via nonmagnetic metal such as Ru or Cu to reduce H_{start} .¹² Up to now, we have considered the case of a 5 nm nonmagnetic layer with the interlayer exchange coupling $J = 0$; we now consider the case of $J = 0.03$ erg/cm² assuming a 3.0 nm thick Cu layer. While stronger ferromagnetic J leads to further decrease in H_{start} within the single domain model, our micromagnetic simulations revealed that ferromagnetic $J > 0.03$ erg/cm² causes the formation of complex magnetic domain structure, and thus it is difficult to keep the antiparallel configuration between the ferromagnetic layers at the remanent state. Figure 7 shows the operating field margin windows for the circular cylinder cell and TD cells ($A = B = 25$ and 45 nm) of the layer structure CoFe (2.5 nm)/Cu (3.0 nm, $J = 0.03$ erg/cm²)/CoFe (2.4 nm). For the circular cylinder, the window is asymmetric, i.e., the minimum critical field for the word field is much larger than that for the digit field because of the formation of S -type edge

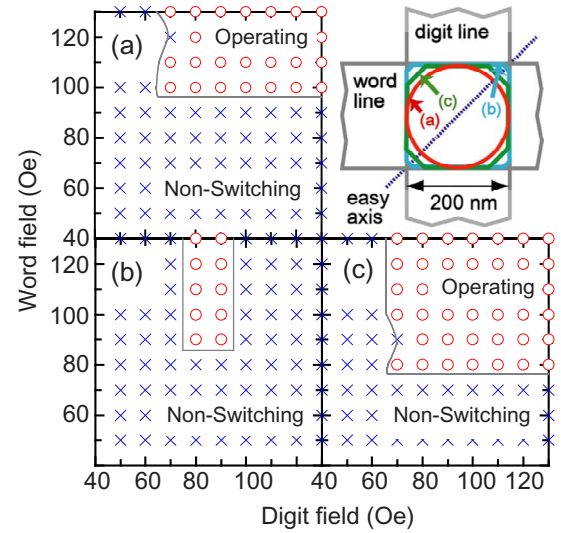


FIG. 7. (Color online) Operation window of toggle-writing for (a) circular cylinder, (b) TD ($A = B = 25$ nm), and (c) TD ($A = B = 45$ nm) cells. Circle and cross show successful switching and no switching, respectively.

domains. The unsuccessful toggle switching at a small field near H_{start} is caused by the unswitched magnetization around the edges after the first H_{word} is applied. Therefore, higher H_{word} is necessary to switch the magnetization in the toggle-mode writing procedure. In the case of TD, as expected from the results shown in Fig. 3, $L_{\text{trim}} = 45$ nm gives a much greater margin with smaller minimum critical fields than for $L_{\text{trim}} = 25$ nm.

Further decrease in the required minimum critical field for toggle switching is found to be attainable by asymmetric trimming of the points for TD cells, as shown in Fig. 8. While previously we used equal trimmed edge lengths $A = B = 45$ nm, in shape (b) in Fig. 8, we decrease B to 25 nm, keeping A equal to 45 nm. The easy axis diagonal length remains 237.8, but the hard-axis length increases to 257.8

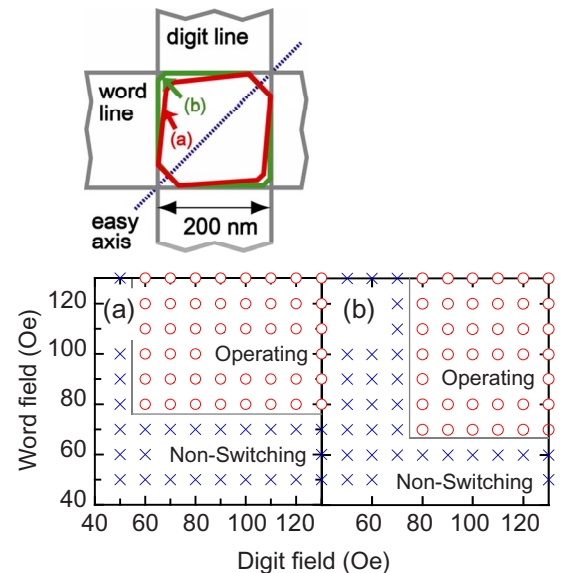


FIG. 8. (Color online) Operation window of toggle-writing for asymmetric TD ($A = 45$ nm and $B = 25$ nm) cells with diagonal length of (a) 237.8 and (b) 257.8 nm along the hard axis. Circle and cross show successful switching and no switching, respectively.

nm. We consider also another shape (a) in which the diagonals are made equal again by shrinking the system along the hard axis to make both diagonal lengths equal to 237.8 nm. For shape (a), the minimum H_{digit} for the toggle switching is decreased. On the other hand, for shape (b), the minimum H_{word} is decreased, while the minimum H_{digit} is increased. The main difference in the magnetic parameters between these asymmetrically trimmed cells and the original cell is their shape anisotropy. Actually, analytic study using a single domain model shows that with the increase in the ratio of the anisotropy field to the antiferromagnetic coupling field between the two magnetic layers composing the SAF, the minimum H_{word} increases monotonically, while the minimum H_{digit} increases at first but at a critical value of the ratio it starts to decrease. (Details will be presented elsewhere.) This means that with the increase in H_k , there exists some critical value depending on H_{couple} at which the anisotropy starts to aid, in cooperation with H_{word} , the clockwise rotation of the net moment at the second step of the toggle switch process when H_{digit} is applied. Actually, the total anisotropy of the present model is smaller than the critical value predicted by the single domain model. However, the magnetization of the present model behaves considerably differently from that of the single domain model, as was discussed above. Therefore, the decrease and increase in the minimum H_{digit} for (a) and (b) compared with the original cell with $A=B=45$ nm may be attributed to the increase and decrease in the shape anisotropy for (a) and (b) compared with the original cell, although further study is still necessary for the full understanding of the above phenomenon.

It should be noted that the critical field for the switching is easily decreased if we neglect the thermal stability of the memory cell. The energy barrier of the memory cell can be expressed as

$$K^*V = [K_u + (1-r)K_{\text{sh}}]V, \quad (5)$$

with

$$K_{\text{sh}} = \frac{1}{2}(N_y - N_x)M_s^2, \quad (6)$$

where K_u is the intrinsic uniaxial magnetic anisotropy constant, V is the volume, N_x and N_y are demagnetizing factors in the x and y directions, and M_s is the saturation magnetization. The demagnetizing factor of the TD cells is determined by micromagnetic simulations. The energy barriers of shapes (a) and (b) were $80k_B T$ (4.44×10^{-12} erg) and $64k_B T$ (3.53×10^{-12} erg), respectively. The shorter length along the hard axis increases the shape anisotropy for the TD cell. The required energy barrier of the magnetic memory cell is $61k_B T$ (3.37×10^{-12} erg) for 10 year lifetime ($T=400$ K, the number of the cells= 10^{12} , and the frequency factor= 10^9 s $^{-1}$).³ Therefore, both cell shapes have enough thermal barrier for

the MRAM application. However, in order to discuss the pure shape effect, we have done the toggle-switching simulations for shape (b) with the same energy barrier as shape (a) by increasing the intrinsic uniaxial magnetic anisotropy. The required minimum word and digit fields for the toggle switching were drastically increased to 80 and 110 Oe, respectively. Therefore, the asymmetric TD shown in Fig. 8(a) could be the optimal shape for 200 nm cells for the toggle MRAM application.

IV. CONCLUSIONS

Micromagnetic simulations of the memory cells for high-density toggle MRAM were performed. While a small aspect ratio and a weak antiferromagnetic coupling between the magnetic layers comprising the SAF are necessary to reduce the minimum field for toggle switching, such a memory cell forms edge domains, increasing the switching field. The formation of edge domains is suppressed by a sharp point, e.g., a diamond shape. However, the sharp points at which the demagnetizing field is low must be trimmed off to attain a reasonable operating field margin. The optimal trimming of the points has been found to be asymmetric: the trimmed edge length is 45 and 25 nm for the easy and hard axes, respectively, with the same diagonal length of 237.8 nm. The minimum toggle-switching field is drastically decreased compared to the conventional circular cylinder cell. The TD shaped cell gives a reasonable write field window as well as the thermal stability required for magnetic memory and thus is suitable for future high-density toggle MRAM.

ACKNOWLEDGMENTS

This work was supported in part by the National Science foundation MRSEC under Grant No. DMR-0213985. Y.F. is supported by JSPS Postdoctoral Fellowships for Research Abroad.

¹L. Savtchenko, A. A. Korin, B. N. Engel, N. D. Rizzo, M. F. Deherra, and J. A. Janesky, U.S. Patent No. 6,545,906 B1 (8 April 2003).

²See www.freescale.com

³H. Fujiwara, S.-Y. Wang, and M. Sun, *Trans. Magn. Soc. Jpn.* **4**, 121 (2004).

⁴D. C. Worledge, *Appl. Phys. Lett.* **84**, 2847 (2004).

⁵D. C. Worledge, *Appl. Phys. Lett.* **84**, 4559 (2004).

⁶H. Fujiwara, S.-Y. Wang, and M. Sun, *J. Appl. Phys.* **97**, 10P507 (2005).

⁷S.-Y. Wang and H. Fujiwara, *J. Appl. Phys.* **98**, 024510 (2005).

⁸D. C. Worledge, P. L. Trouilloud, M. C. Gaidis, Y. Lu, D. W. Abraham, S. Assefa, S. Brown, E. Galligan, S. Kanakasabapathy, J. Nowak, E. Osullivan, R. Robertazzi, G. Wright, and W. J. Gallagher, *J. Appl. Phys.* **100**, 074506 (2006).

⁹Y. Fukuma, H. Fujiwara, and P. B. Visscher, *J. Appl. Phys.* **103**, 07A716 (2008).

¹⁰M. Scheinfein (<http://llgmicro.home.mindspring.com>).

¹¹S. S. P. Parkin, *Phys. Rev. Lett.* **67**, 3598 (1991).

¹²D. W. Abraham and D. C. Worledge, *Appl. Phys. Lett.* **88**, 262505 (2006).